Обзор ArXiv:astro-ph, март 27-31, 2017

От Сильченко О.К.

Astro-ph: 1703.08410

DRAFT VERSION MARCH 27, 2017
Preprint typeset using LATEX style emulateapj v. 12/16/11

CORE OR CUSPS: THE CENTRAL DARK MATTER PROFILE OF A REDSHIFT ONE STRONG LENSING CLUSTER WITH A BRIGHT CENTRAL IMAGE

THOMAS E. COLLETT[1], ELIZABETH BUCKLEY-GEER[2], HUAN LIN[2], DAVID BACON[1], ROBERT C. NICHOL[1], BRIAN NORD[2], XAN MORICE-ATKINSON[1], ADAM AMARA[3], SIMON BIRRER[4,3], NIKOLAY KUROPATKIN[2], ANUPREETA MORE[5], CASEY PAPOVICH[6], KATHY K. ROMER[7], NICOLAS TESSORE[8], TIM M. C. ABBOTT[9], SAHAR ALLAM[2], JAMES ANNIS[2], AURLIEN BENOIT-LÉVY[10,11,12], DAVID BROOKS[11], DAVID L. BURKE[13,14], MATIAS CARRASCO KIND[15,16], FRANCISCO JAVIER J. CASTANDER[17], CHRIS B. D'ANDREA[18], LUIZ N. DA COSTA[19,20], SHANTANU DESAI[21], H. THOMAS DIEHL[2], PETER DOEL[11], TIM F. EIFLER[22,23], BRENNA FLAUGHER[2], JOSH FRIEMAN[2,24], DAVID W. GERDES[25,26], DANIEL A. GOLDSTEIN[27,28], DANIEL GRUEN[13,14], JULIA GSCHWEND[19,20], GASTON GUTIERREZ[2], DAVID J. JAMES[29,9], KYLER KUEHN[30], STEVE KUHLMANN[31], OFER LAHAV[11], TING S. LI[2,6], MARCOS LIMA[32,19], MARCIO A. G. MAIA[19,20], MARISA MARCH[18], JENNIFER L. MARSHALL[6], PAUL MARTINI[33,34], PETER MELCHIOR[35], RAMON MIQUEL[36,37], ANDRS A. PLAZAS[23], ELI S. RYKOFF[13,14], EUSEBIO SANCHEZ[38], VIC SCARPINE[2], RAFE SCHINDLER[14], MICHAEL SCHUBNELL[26], IGNACIO SEVILLA-NOARBE[38], MATHEW SMITH[39], FLAVIA SOBREIRA[40,19], ERIC SUCHYTA[41], MOLLY E. C. SWANSON[16], GREGORY TARLE[26], DOUGLAS L. TUCKER[2], ALISTAIR R. WALKER[9]

[1]Institute of Cosmology & Gravitation, University of Portsmouth, Portsmouth, PO1 3FX, UK
[2]Fermi National Accelerator Laboratory, P. O. Box 500, Batavia, IL 60510, USA
[3]Department of Physics, ETH Zurich, Wolfgang-Pauli-Strasse 16, CH-8093 Zurich, Switzerland
[4]Department of Physics and Astronomy, UCLA, PAB, 430 Portola Plaza, Box 951547, Los Angeles, CA 90095-1547, USA
[5]Kavli IPMU (WPI), UTIAS, The University of Tokyo, Kashiwa, Chiba 277-8583, Japan
[6]George P. and Cynthia Woods Mitchell Institute for Fundamental Physics and Astronomy, and Department of Physics and Astronomy, Texas A&M University, College Station, TX 77843, USA
[7]Department of Physics and Astronomy, Pevensey Building, University of Sussex, Brighton, BN1 9QH, UK
[8]Jodrell Bank Center for Astrophysics, School of Physics and Astronomy, University of Manchester, Oxford Road, Manchester, M13 9PL, UK
[9]Cerro Tololo Inter-American Observatory, National Optical Astronomy Observatory, Casilla 603, La Serena, Chile
[10]CNRS, UMR 7095, Institut d'Astrophysique de Paris, F-75014, Paris, France

Далекое скопление галактик на z=1

- Изначально объект взят из обзора SPT (South-Pole Telescope) – поиск скоплений галактик по эффекту Сюняева-Зельдовича.
- В данной работе – фотометрия с DES и спектроскопия всего, что в поле, на GMOS.

Галактики (красные) и дуги заднего фона (голубые)

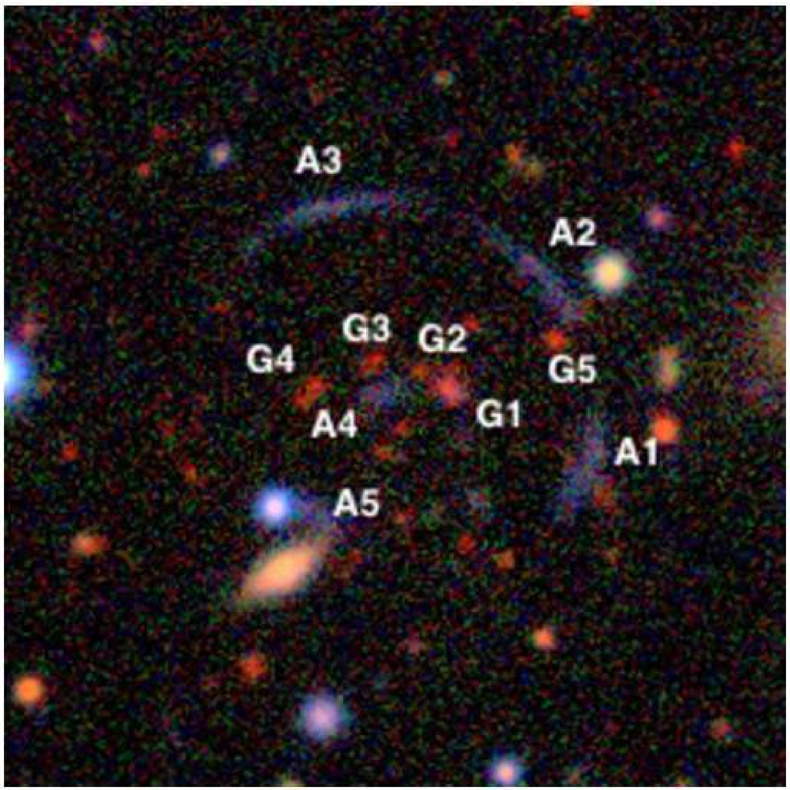

FIG. 1.— Pseudo-colour *gri* composite image of the lens J2011, taken from the first three years of operation of DES. The image is 1 arcminute on a side.

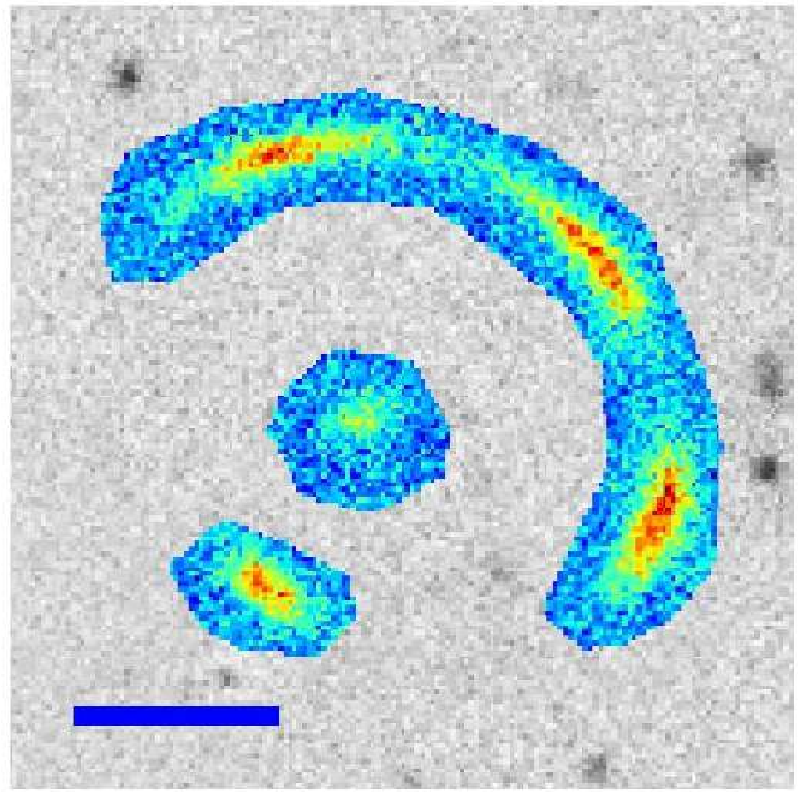

FIG. 2.— *g* band image of the arcs and central image, after subtracting foregrounds. Only the coloured pixels are included in the lens modelling of Section 3. The blue bar shows a ten arcsecond scale.

Object	RA	DEC	Redshift	R-value
A2	302.777796	-52.468769	2.3875 ± 0.0002	4.62
A3	302.785149	-52.467079	2.3889 ± 0.0002	5.34
A4	302.783661	-52.471130	2.3875 ± 0.0004	2.26

TABLE 3
REDSHIFTS FOR G1-G5

Object	RA	DEC	Redshift
G1	302.78122	-52.47105	1.0645 ± 0.0002
G2	302.78244	-52.47035	1.0737 ± 0.0002
G3	302.78418	-52.47032	1.0642 ± 0.0002
G4	302.78605	-52.47087	1.0514 ± 0.0002
G5	302.77766	-52.46994	1.0684 ± 0.0002

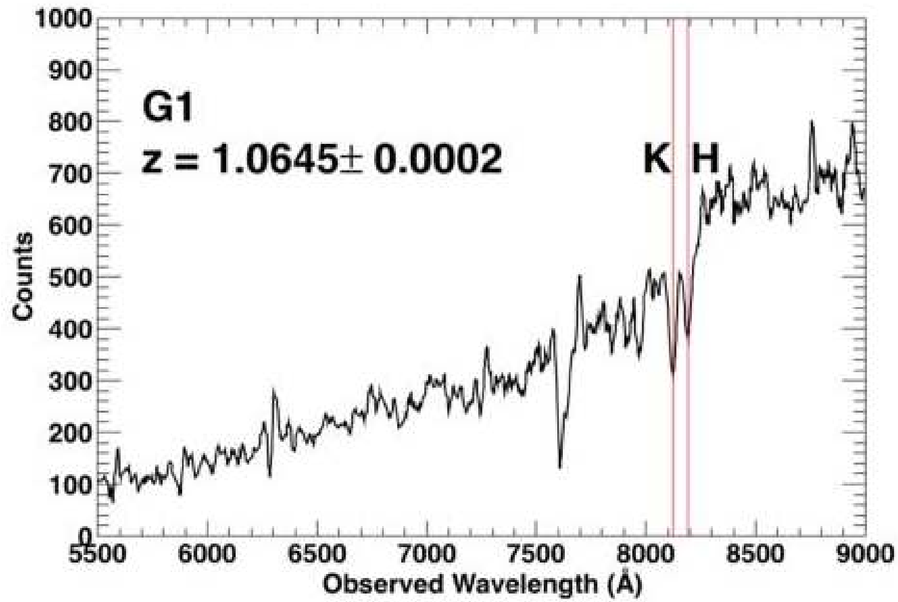

FIG. 4.— The extracted un-fluxed 1-D spectra for the BCG (G1).

Модель сильного линзирования одним темным гало - CORE

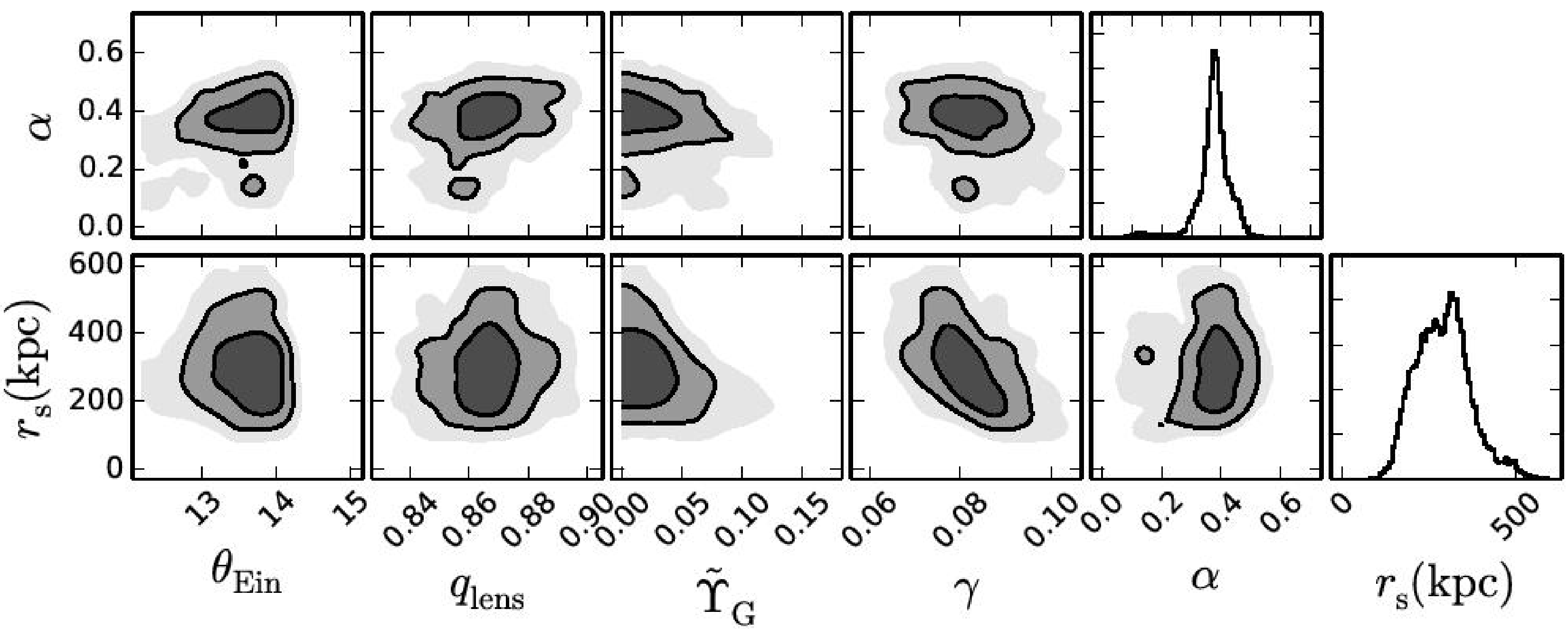

FIG. 8.— The marginalized 1 and 2 dimensional parameter constraints for the single dark matter halo model of J2011. The contours show the 68, 95 and 99 percent confidence regions respectively. $\theta_{\rm E}$ is the Einstein radius of the DM halo [a]. The flattening of the DM halo is $q_{\rm lens}$, α is the inner profile slope and $r_{\rm s}$ (kpc) is the scale radius of the gNFW halo. $\tilde{\Upsilon}_{\rm G}$ relates the observed z-band fluxes and the Einstein radiis of the cluster members, it is in units such that $\tilde{\Upsilon}_{\rm G}$ is the Einstein radius of the BCG in arcseconds. The inner profile slope and the scale radius of the gNFW halo have only a mild covariance with the unshown parameters of the model.

[a]Not the total Einstein radius of the arcs - since this is made up from the DM and the cluster members

Сильное грав. линзирование ДВУМЯ гало – может быть и NWF

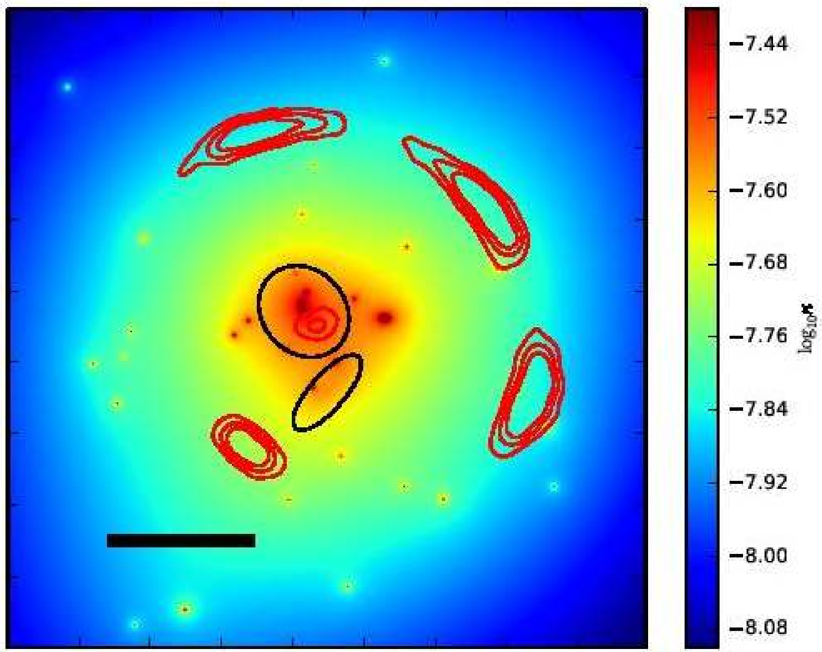

FIG. 11.— The mass distribution in J2011 as inferred from the two DM halo model. The red contours show the location of the lensed images. The black ellipses indicate the locations and flattenings of the two DM halos. The black bar indicates a 10 arcsecond scale.

Astro-ph: 1703.09446

MNRAS 000, 1–?? (...) Preprint 29 March 2017 Compiled using MNRAS LaTeX style file v3.0

Is ram-pressure stripping an efficient mechanism to remove gas in galaxies?

Vicent Quilis[1,2⋆], Susana Planelles[1], Elena Ricciardelli[3]
[1] *Departament d'Astronomia i Astrofísica, Universitat de València, c/ Dr. Moliner 50, E-46100 - Burjassot, València, Spain*
[2] *Observatori Astronòmic, Universitat de València, E-46980 Paterna, València, Spain*
[3] *Laboratoire d'Astrophysique, École Polytechnique Fédérale de Lausanne (EPFL), 1290 Sauverny, Switzerland*

Содержание и холодного, и горячего СВЯЗАННОГО газа растет со временем – за счет аккреции из ICM

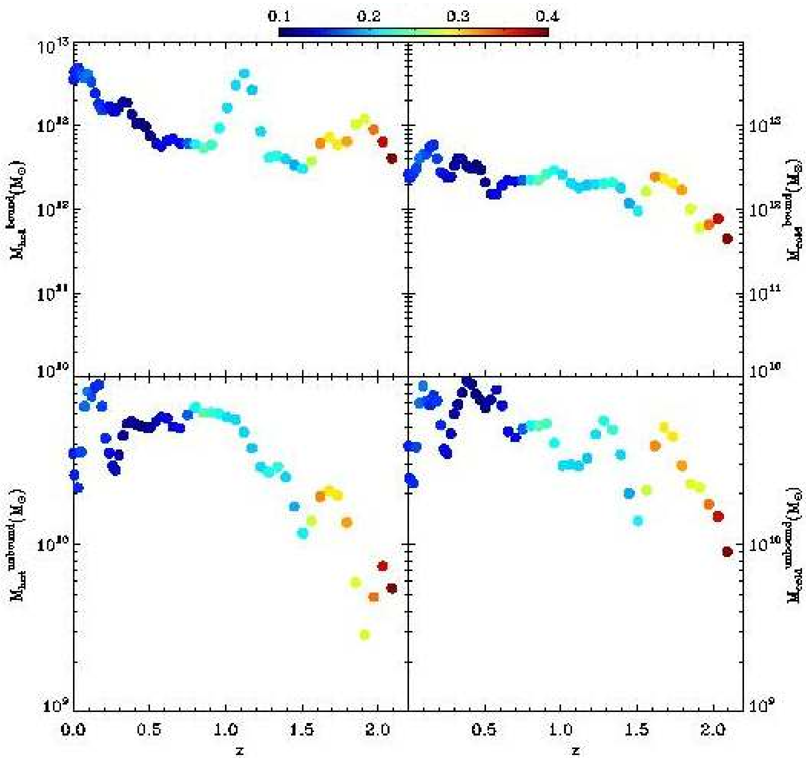

Figure 9. Evolution of the gaseous mass content (bound and unbound) averaged for all galaxies whose history can be tracked back from $z \sim 0$ to $z \sim 2$. The masses of the four gas components, namely, hot ($T > 5 \times 10^4$ K) bound gas (top-left panel), cold ($T < 5 \times 10^4$ K) bound gas (top-right), hot unbound gas (bottom-left), and cold unbound gas (bottom-right) are displayed. At a

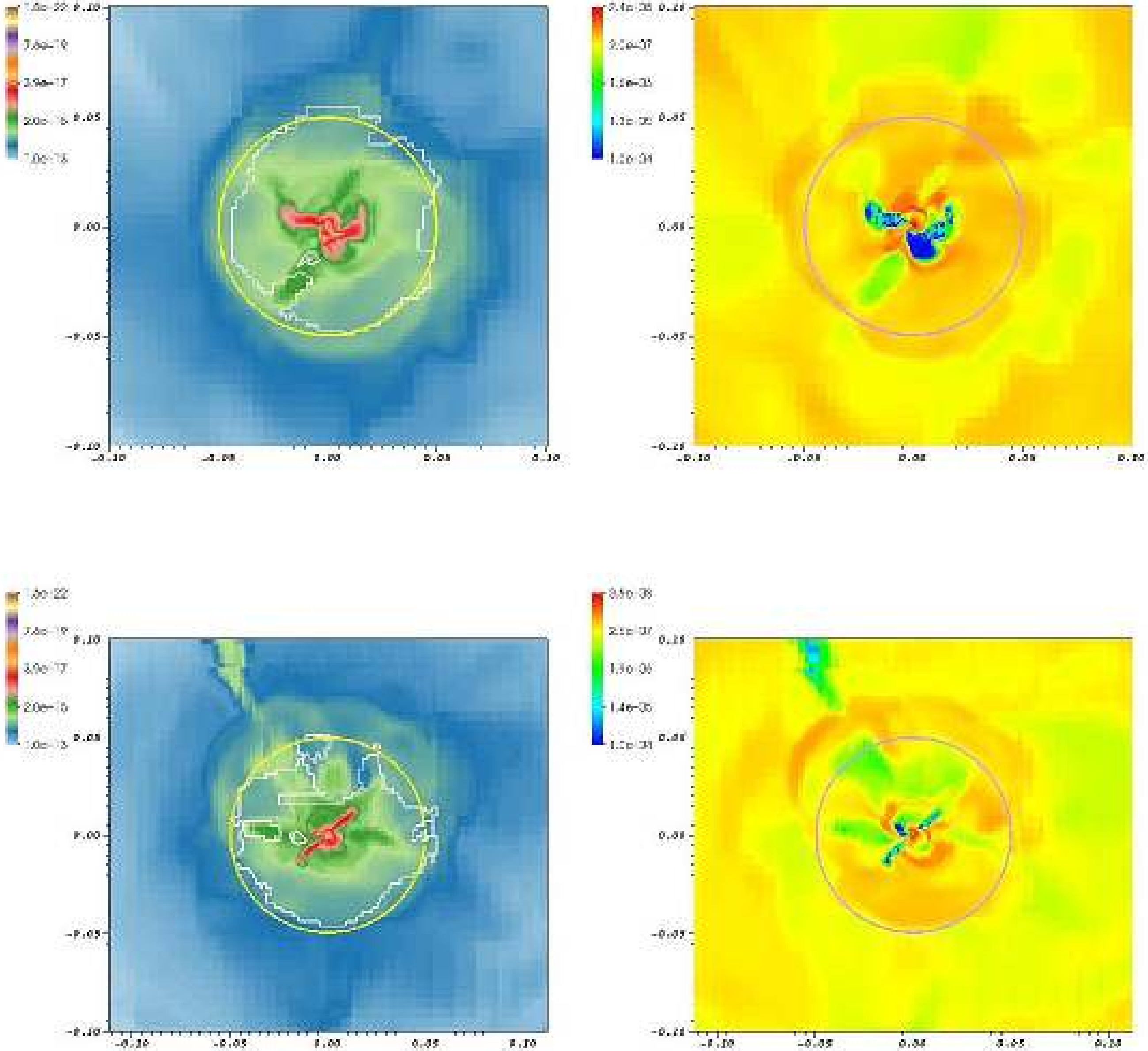

Figure 11. Density (left panels) and temperature (right panels) of the gas in a thin slice through the centre of one of the best numerically resolved galaxies in the simulation at $z \sim 0$. The upper (lower) panels represent a face-on (edge-on) view of the galaxy. The density (temperature) of the gas is in units of $M_{\odot}/Mpc^3$ (K). The yellow and purple circles mark the radius of the galactic halo. The white contour defines the boundary between bound and unbound gas.The axis of the panels are in units of Mpc.

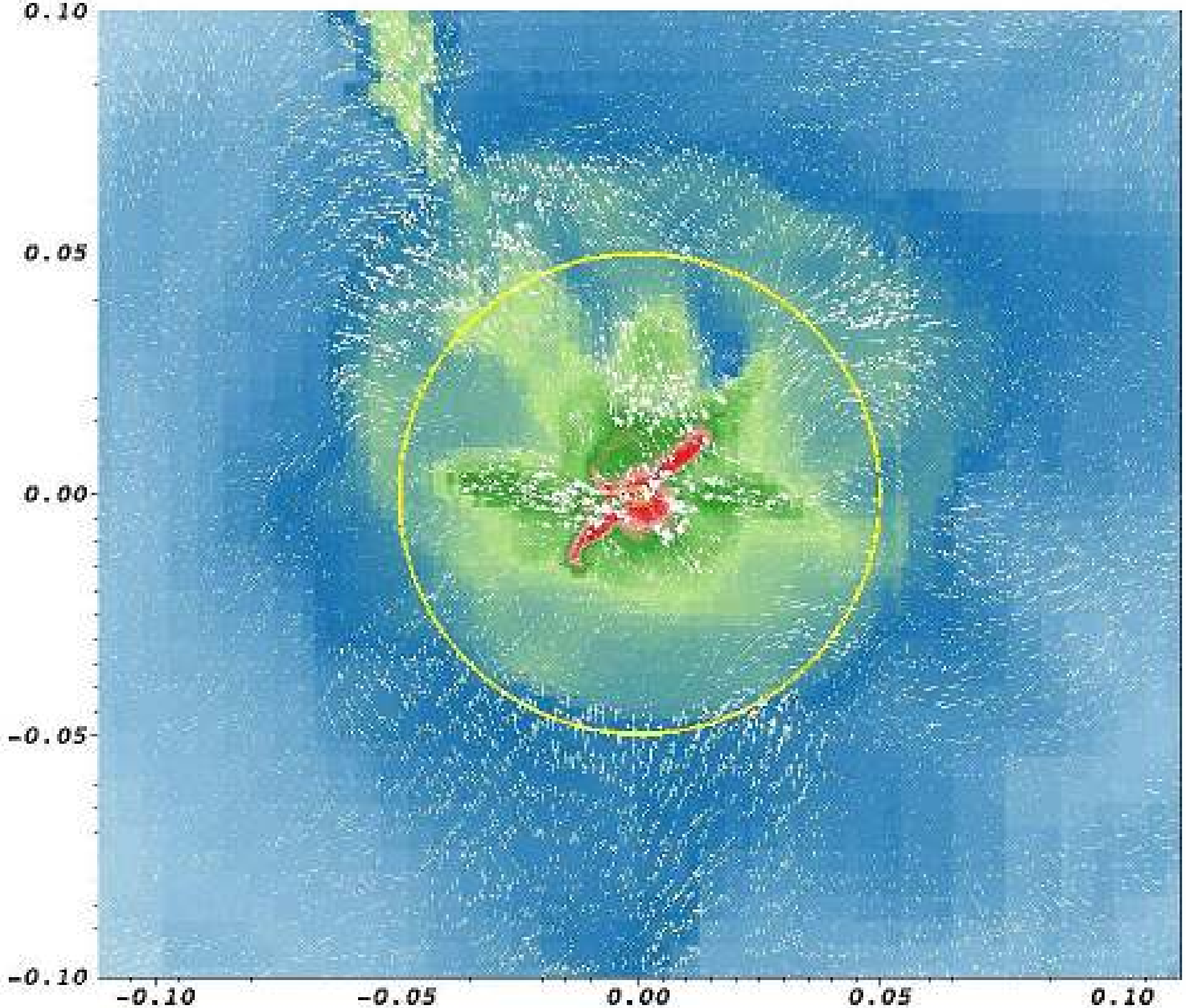

Figure 12. Gas density in a thin slice through the centre of a galaxy from a edge-on view. Superimposed to the density map, the velocity field of the gas is shown as white vectors whose size is scaled according to their magnitudes. The galaxy is moving towards the right lower corner of the image. The axis of the panels are in units of Mpc. The velocity frame of reference is the centre of the computational box

Выводы

The existence of a complex pattern of flows, turbulence and a constant fueling of gas to the hot corona from the ICM could produce, according to the results presented in this paper, that the global effect of the interaction of the galaxies with their environment could be substantially less dramatic than suggested in earlier works. In these references, it is mostly accepted that the hot corona can be quickly swept away in scales of few Myrs (e.g. McCarthy et al. 2008; Vijayaraghavan & Ricker 2015) and that the cold component is also dramatically affected but on larger temporal scales (e.g. Quilis et al. 2000). However, the results presented in this paper show that all galaxies retain an important fraction of bound gas, both hot and cold, being in all cases the hot bound component dominant. These striking results would be in agreement with the observational results (e.g. Sun et al. 2007; Jeltema et al. 2008; Goulding et al. 2016) evidencing that all observed galaxies exhibit a hot galactic corona. Mulchaey & Jeltema (2010) suggested that the temperature gradient between the hotter gas in the ICM and the relatively cooler gas in the corona would translate into a pressure gradient competing with the RPS. The results presented in this paper could be explained by a combination of these two effects: on the one side, the confining action of the temperature gradient between the ICM and the cooler external part of the galactic halo and, on the other side, the gas flows from the ICM that continuously percolate the corona and, therefore, reduce the relevance of the interaction with the environment.

Astro-ph: 1703.09345

HALOGAS OBSERVATIONS OF NGC 4559: ANOMALOUS AND EXTRA-PLANAR H I AND ITS RELATION TO STAR FORMATION

Carlos J. Vargas[1], George Heald[2,3,4], René A.M. Walterbos[1], Filippo Fraternali[4,5], Maria T. Patterson[6], Richard J. Rand[7], Gyula I. G. Józsa[8,9,10], Gianfranco Gentile[11], Paolo Serra[12]

[1]Department of Astronomy, New Mexico State University, Las Cruces, NM 88001

[2]CSIRO Astronomy and Space Science, 26 Dick Perry Ave, Kensington WA 6151 Australia

[3]The Netherlands Institute for Radio Astronomy (ASTRON), Dwingeloo, The Netherlands

[4]Kapteyn Astronomical Institute, University of Groningen, Postbus 800, 9700 AV Groningen, The Netherlands

[5]Dept. of Physics and Astronomy, University of Bologna, Viale Berti Pichat 6/2, 40127, Bologna, Italy

[6]Department of Astronomy, University of Washington, Box 351580, Seattle, WA 98195

[7]Department of Physics and Astronomy, University of New Mexico, 1919 Lomas Blvd. NE, Albuquerque, NM 87131

[8]SKA South Africa Radio Astronomy Research Group, 3rd Floor, The Park, Park Road, Pinelands 7405, South Africa

[9]Rhodes Centre for Radio Astronomy Techniques & Technologies, Department of Physics and Electronics, Rhodes University, PO Box 94, Grahamstown 6140, South Africa

[10]Argelander-Institut für Astronomie, Auf dem Hügel 71, D-53121 Bonn, Germany

[11]Department of Physics and Astrophysics, Vrije Universiteit Brussel, Pleinlaan 2, 1050 Brussels, Belgium

[12]INAF Osservatorio Astronomico di Cagliari, Via della Scienza 5, I-09047 Selargius (CA), Italy

Галактика позднего типа, наклоненная под промежуточным углом

Parameter	Value
Hubble Type	SABcd
Adopted Distance	7.9 Mpc ($1'' = 38.3$ pc)
M_B	-20.07
D_{25}	$11.3'$
v_{max}	~ 130 km s^{-1}
Total Mass (Virial)	$\sim 2.8 \times 10^{11}$ $M_\odot$

Table 1. Parameters of NGC 4559. The total mass was computed using Klypin et al. (2011), and represents the virial mass of NGC 4559.

HI-наблюдения в Вестерборке с разрешением около 30’’

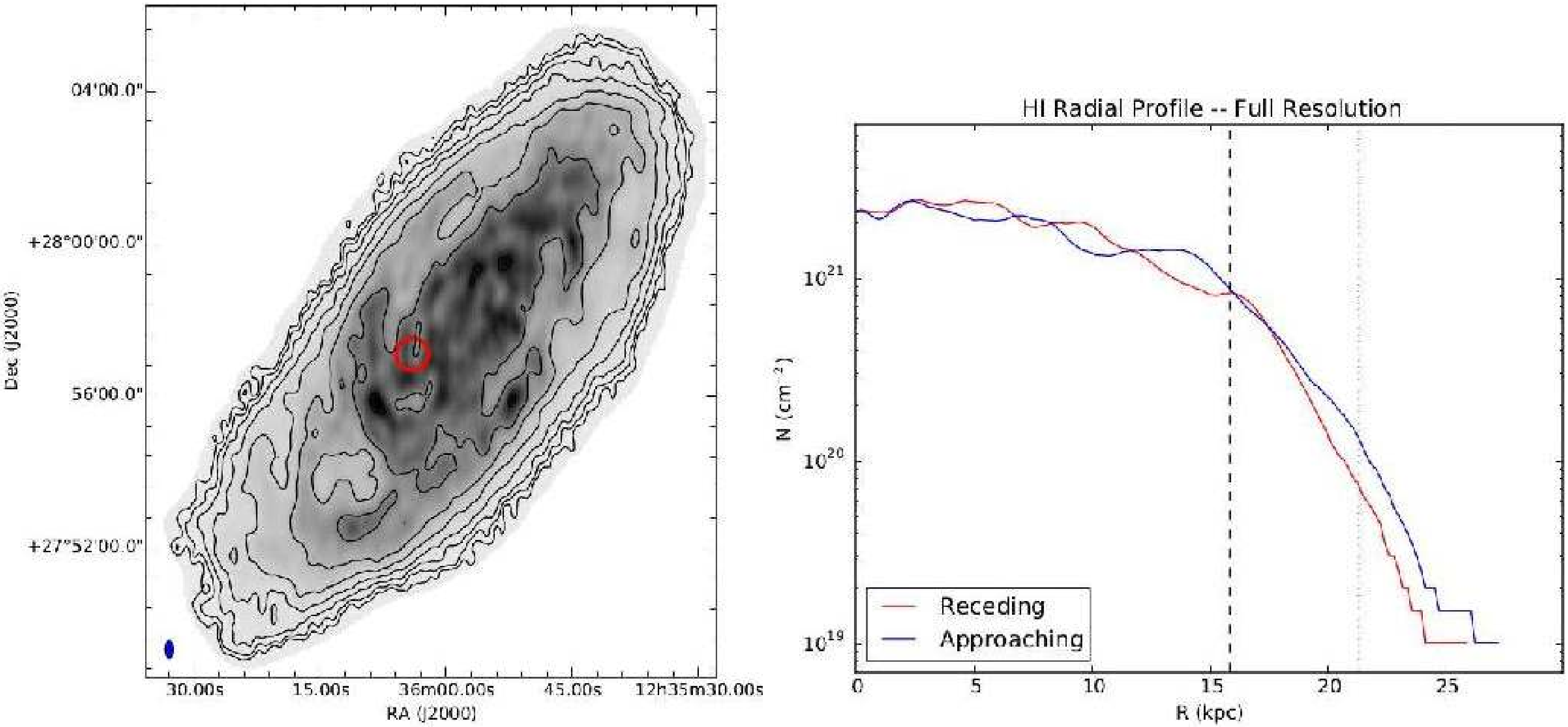

Figure 1. Left: Integrated H I map of the highest resolution HALOGAS data cube for NGC 4559. Column density contours begin at 2.4×10^{19} atoms cm^{-2} and increase in multiples of 2. The red circle marks the location of an H I hole discussed further in Section 5.2. Right: Radial profile obtained from the highest resolution integrated H I map. The vertical dashed line represents R_{25} of the galaxy, and the dotted vertical line is the largest radius at which B05 detects H I, as quoted in that text, and adjusted to our assumed distance of 7.9 Mpc.

Тонкий диск видели и раньше, но в глубоких изображениях стало видно и толстый HI-диск

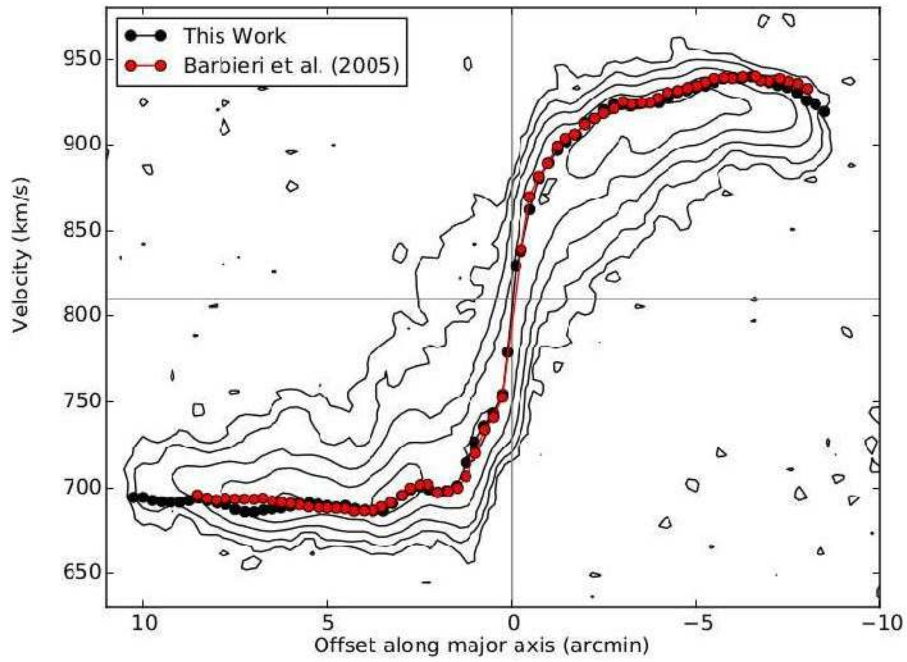

Figure 4. Rotation curves of the best fitting thin disk model (black) and the model of Barbieri et al. (2005) (red) overlaid atop the position-velocity slice along the major axis. Contours begin at 2σ and increase in multiples of 3. From left to right, this figure moves along the major axis following from south-east to north-west as seen on the sky. Rotation curve values are shown at the inclination of the galaxy. A gas feature at forbidden velocity can be seen in the top-left quadrant and is discussed further in Section 5.2.

Когда вычли тонкий диск и оставили один старый – стало видно, что его сделали фонтаны

Parameter	Uniform Lag Model	Fine-tuned Model
Thin Disk Scale Height pc	200 pc	200 pc
Thick Disk Scale Height	2 kpc	2 kpc
Central Position Angle	$-37.0°$	$-37.0°$
Central Inclination	$67.2°$	$67.2°$
Kinematic Center (α, δ, J2000)	$12^h35^m58^s$ $+27°57'32''$	$12^h35^m58^s$ $+27°57'32''$
Thick Disk Lag Magnitude	Approaching:13; Receding: 6.5 km s^{-1} kpc^{-1}	Approaching: 13; Receding: $0-13$ km s^{-1} kpc^{-1}
Global Velocity Dispersion	10 km s^{-1}	10 km s^{-1} + $(0-15)$ km s^{-1}
Percentage Gas in Thick Disk	20%	20%
Vertical Density Profile	$sech^2 + sech^2$	$sech^2 + sech^2$

Table 3. Tilted Ring Fitting Parameters of NGC 4559. Central position angle describes the inner, unwarped section of the disk. The fine-tuned model contains all of the same global properties as the Thin + Thick Disk Model, and has variable values for thick disk lag magnitude and velocity dispersion. See the text for details on variable parameters in the fine-tuned model.

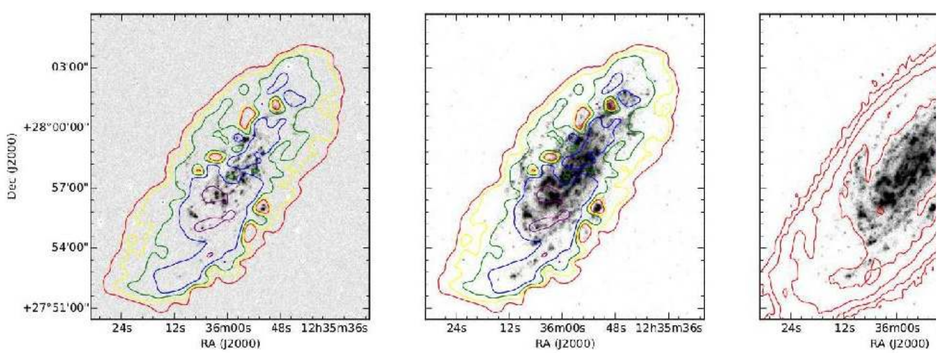

Figure 7. Left: KPNO Hα image, middle: GALEX FUV image (Gil de Paz et al. 2007), right: Galex FUV imag atop the left two images are the total extracted extra-planar gas moment 0 contours. The colors represent differe column density and range, from lowest to highest, red, yellow, green, blue, and violet. The contours begin at 3.75 × cm^{-2} and increase in multiples of 2. Overlaid atop the rightmost image is the full resolution HI data, the same as

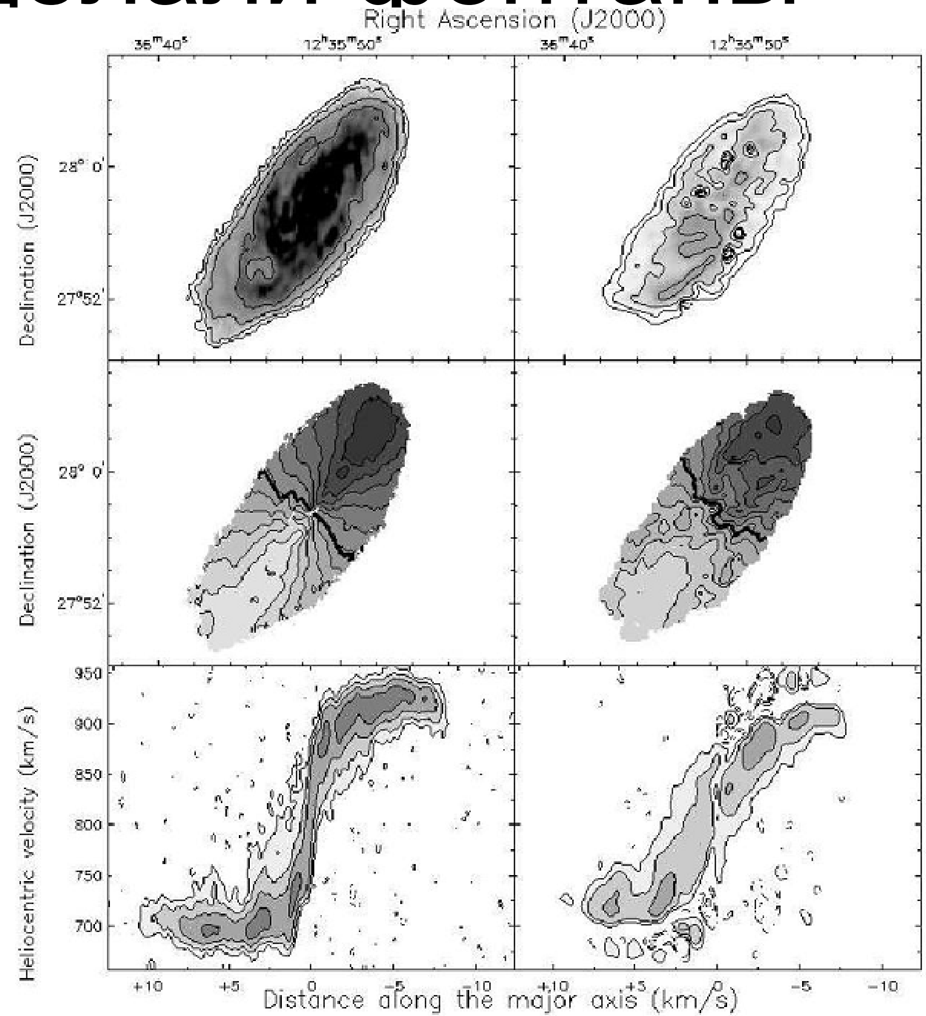

3. Various plots of the extra-planar gas extraction results. Upper left: Integrated HI map of the data.

Astro-ph: 1703.09769

The Mass-Metallicity Relation revisited with CALIFA

S.F. Sánchez[1], J.K. Barrera-Ballesteros[2], L. Sánchez-Menguiano[3,4], C. J. Walcher[5], R. A. Marino[6], L. Galbany[7], J. Bland-Hawthorn[8], M. Cano-Díaz[1], R. García-Benito[3], C. López-Cobá[1], S. Zibetti[9], J.M. Vilchez[3], J. Iglésias-Páramo[3], C. Kehrig[3], A. R. López Sánchez[10,11], S. Duarte Puertas[3], B. Ziegler[12]

[1]*Instituto de Astronomía, Universidad Nacional Autónoma de México, A. P. 70-264, C.P. 04510, México, D.F., Mexico*
[2]*Department of Physics & Astronomy, Johns Hopkins University, Bloomberg Center, 3400 N. Charles St., Baltimore, MD 21218, USA*
[3]*Instituto de Astrofísica de Andalucía (IAA/CSIC), Glorieta de la Astronomía s/n Aptdo. 3004, E-18080 Granada, Spain*
[4]*Departamento de Física Teórica y del Cosmos, University of Granada, Facultad de Ciencias (Edificio Mecenas), E-18071 Granada*
[5]*Leibniz-Institut für Astrophysik Potsdam (AIP), An der Sternwarte 16, D-14482 Potsdam, Germany*
[6]*Department of Physics, Institute for Astronomy, ETH Zürich, CH-8093 Zürich, Switzerland*
[7]*PITT PACC, Department of Physics and Astronomy, University of Pittsburgh, Pittsburgh, PA 15260, USA*
[8]*Sydney Institute for Astronomy, School of Physics, University of Sydney, NSW 2006, Australia*
[9]*INAF-Osservatorio Astrofisico di Arcetri - Largo Enrico Fermi, 5 - I-50125 Firenze, Italy*
[10]*Australian Astronomical Observatory, PO Box 915, North Ryde, NSW 1670, Australia*
[11]*Department of Physics and Astronomy, Macquarie University, NSW 2109, Australia*
[12]*University of Vienna, Department of Astrophysics, Türkenschanzstr. 17, 1180 Vienna, Austria*

Забавное сравнение трех обзоров галактик методом IFU

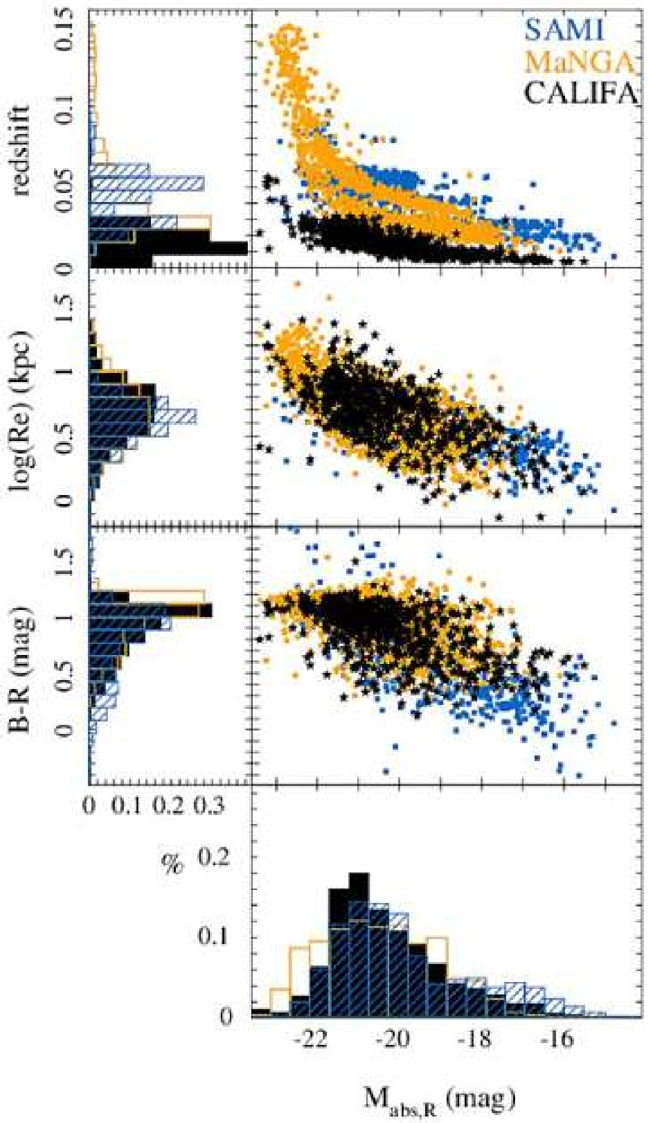

Новая зависимость «масса-металличность» - разные калибраторы дают просто сдвиг по вертикали

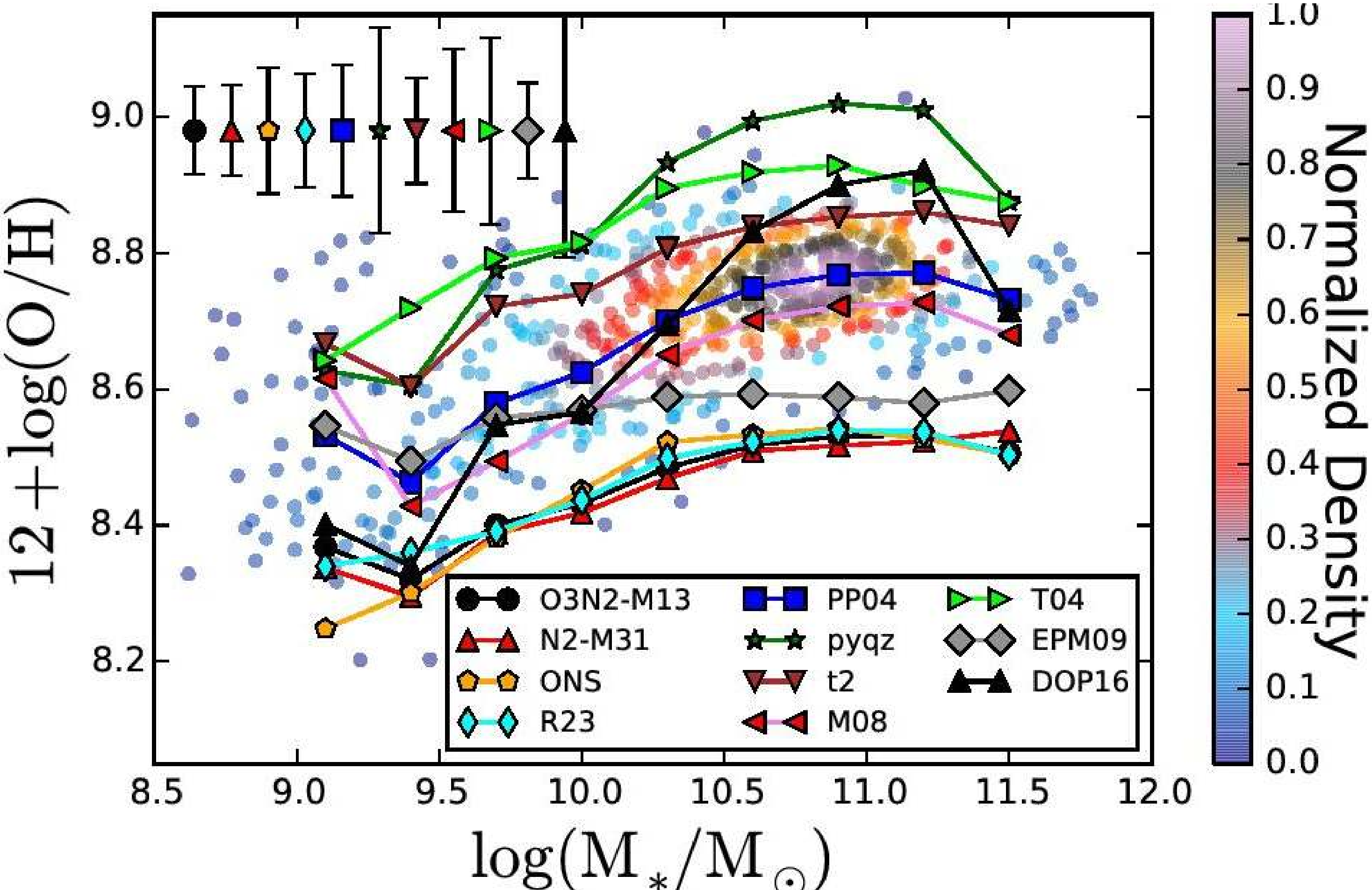

Металличность на эффективном радиусе!

Они утверждают, что закрыли «третью ось» - зависимость металличности от SFR

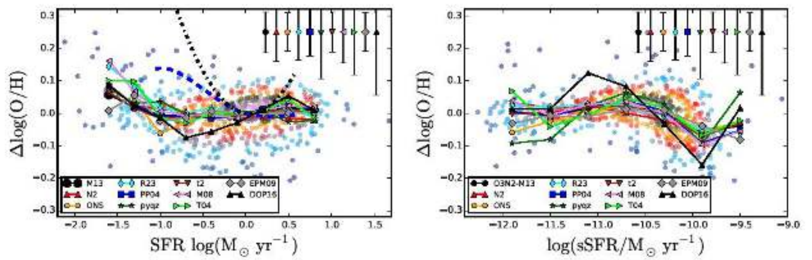

Figure 4. Residuals of the MZ relations from the different analyzed calibrators against the SFR (left-panel) and the sSFR (right-panel). The colored solid circles corresponds to the values derived using the PP04 calibrator, and the line-connected symbols corresponds to median values for each bin and calibrator, following the notation presented in Fig. 3. The error bars in the top-right represent the mean standard deviation of the residuals along the considered bins. The blue-dashed line represents the relation between the residuals and the SFR expected when using the secondary relation proposed by Mannucci et al. (2010), and the black-dotted line represents the same relation when adopted the secondary relation proposed by Lara-López et al. (2010).

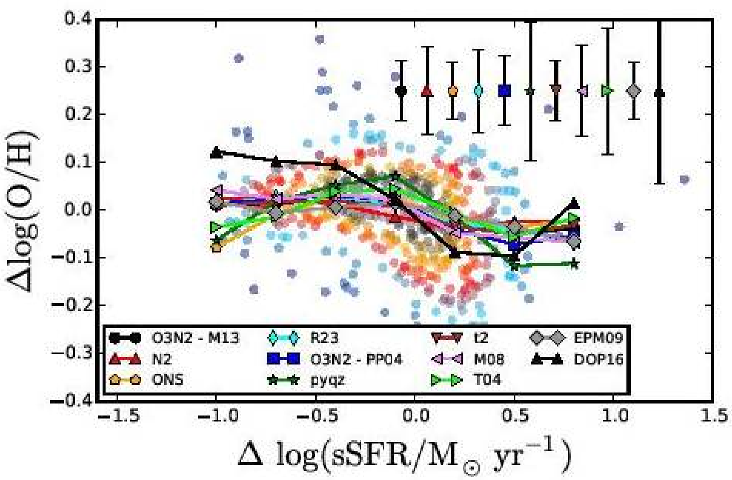

- Но на самом деле, если приглядеться к нижней картинке, то видна НЕ КОРРЕЛЯЦИЯ, но переход в другой режим на высоких темпах SF

Astro-ph: 1703.09724

The VLA-COSMOS 3 GHz Large Project: Cosmic star formation history since $z \sim 5$

M. Novak[1], V. Smolčić[1], J. Delhaize[1], I. Delvecchio[1], G. Zamorani[2], N. Baran[1], M. Bondi[3], P. Capak[4], C. L. Carilli[5], P. Ciliegi[2], F. Civano[6,7], O. Ilbert[8], A. Karim[9], C. Laigle[10], O. Le Fèvre[8], S. Marchesi[11], H. McCracken[10], O. Miettinen[1], M. Salvato[12], M. Sargent[13], E. Schinnerer[14], L. Tasca[8]

[1] Department of Physics, Faculty of Science, University of Zagreb, Bijenička cesta 32, 10000 Zagreb, Croatia
[2] INAF - Osservatorio Astronomico di Bologna, Via Piero Gobetti 93/3, I-40129 Bologna, Italy.
[3] Istituto di Radioastronomia di Bologna - INAF, via P. Gobetti, 101, 40129, Bologna, Italy
[4] Spitzer Science Center, 314-6 Caltech, Pasadena, CA 91125, USA
[5] National Radio Astronomy Observatory, P.O. Box 0, Socorro, NM 87801, USA
[6] Yale Center for Astronomy and Astrophysics, 260 Whitney Avenue, New Haven, CT 06520, USA
[7] Harvard-Smithsonian Center for Astrophysics, 60 Garden Street, Cambridge, MA 02138, USA
[8] Aix Marseille Université, CNRS, LAM (Laboratoire d'Astrophysique de Marseille), UMR 7326, 13388, Marseille, France
[9] Argelander-Institut für Astronomie, Universität Bonn, Auf dem Hügel 71, D-53121 Bonn, Germany
[10] Institut d'Astrophysique de Paris, UMR7095 CNRS, Universit e Pierre et Marie Curie, 98 bis Boulevard Arago, 75014, Paris, France
[11] Department of Physics and Astronomy, Clemson University, Kinard Lab of Physics, Clemson, SC 29634-0978, USA
[12] Max-Planck-Institut für Extraterrestrische Physik (MPE), Postfach 1312, D-85741 Garching, Germany
[13] Astronomy Centre, Department of Physics and Astronomy, University of Sussex, Brighton, BN1 9QH, UK
[14] Max-Planck-Institut für Astronomie, Königstuhl 17, D-69117 Heidelberg, Germany

Новая космическая история звездообразования – по радиоконтинууму

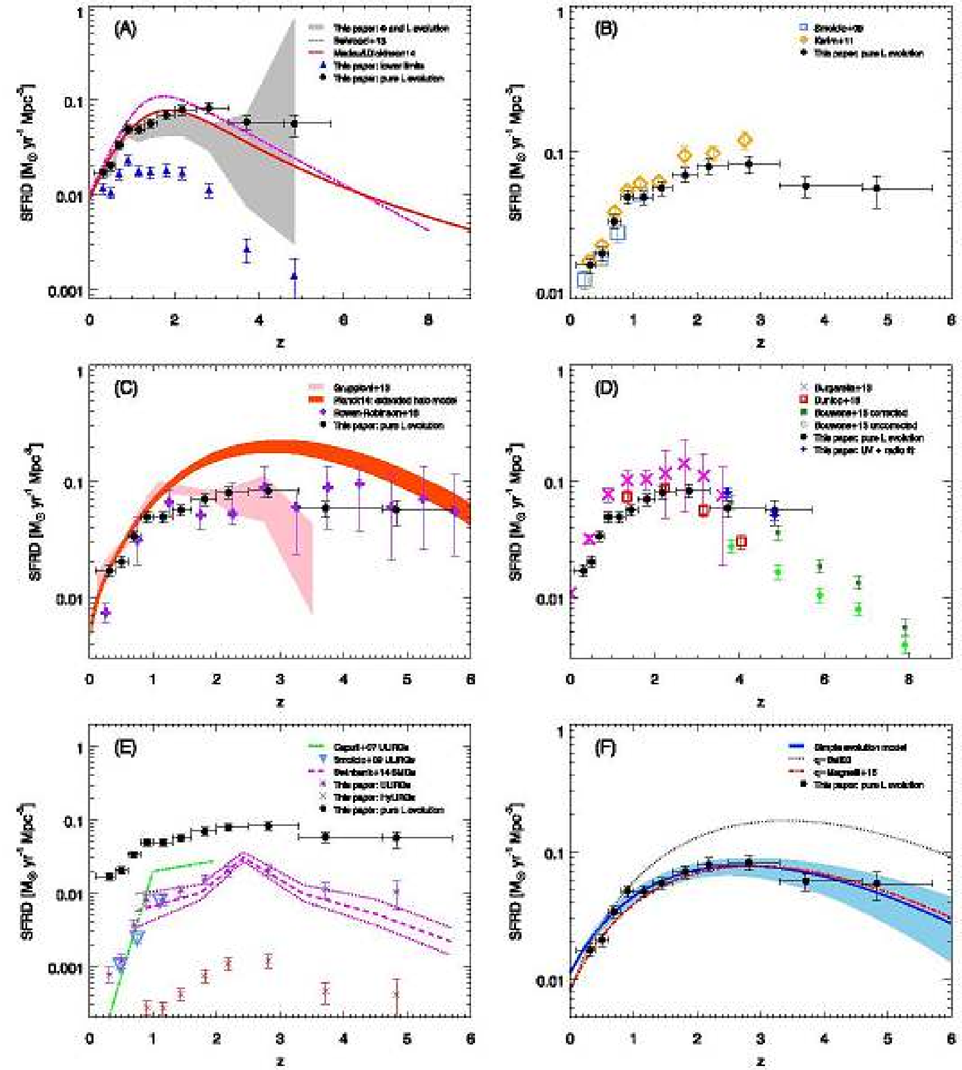

Fig. 6. Cosmic star formation rate density (SFRD) history. Our total SFRD values estimated from the pure luminosity evolution in separate redshift bins are shown as filled black circles in all panels. All data shown for comparison are indicated in the legend of each panel; see text for details.

Astro-ph: 1703.10301

EXTENDED IONIZED GAS CLOUDS IN THE ABELL 1367 CLUSTER [1]

MASAFUMI YAGI[2,3] MICHITOSHI YOSHIDA[4], GIUSEPPE GAVAZZI[5], YUTAKA KOMIYAMA[2,6], NOBUNARI KASHIKAWA[2,6], SADANORI OKAMURA[3,7],
yagi.masafumi@nao.ac.jp
ApJ accepted

ABSTRACT

We surveyed a central 0.6 deg^2 region of Abell 1367 cluster for extended ionized gas clouds (EIGs) using the Subaru prime-focus camera (Suprime-Cam) with a narrow-band filter that covers Hα. We discovered six new EIGs in addition to five known EIGs. We also found that the Hα tail from the blue infalling group (BIG) is extended to about 330 kpc in projected distance, which is about twice longer than previously reported. Candidates of star-forming blobs in the tail are detected. The properties of the EIG parent galaxies in Abell 1367 basically resemble those in the Coma cluster. A noticeable difference is that the number of detached EIGs is significantly fewer in Abell 1367, while the fraction of blue member galaxies is higher. The results suggest a difference in the evolutionary stage of the clusters; Abell 1367 is at an earlier stage than the Coma cluster.

Галактики и облака ионизованного газа

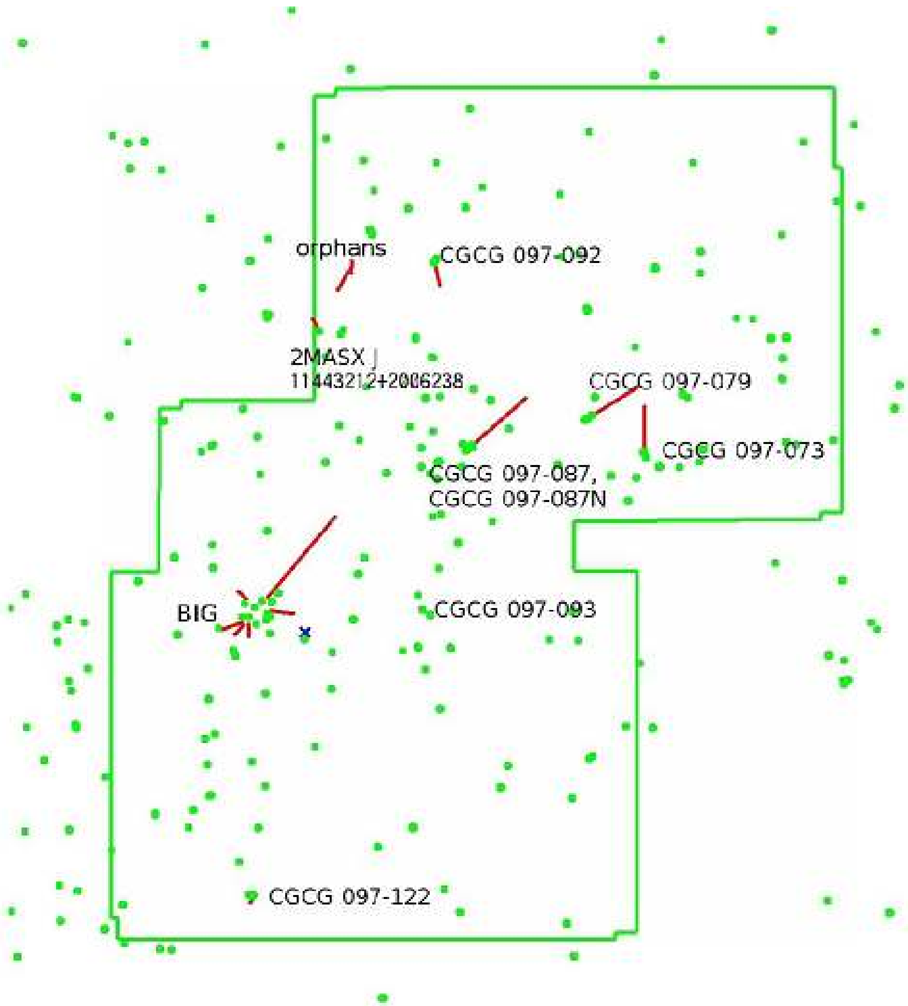

FIG. 5.— Distribution of EIGs. The green dots are spectroscopic member galaxies. The green polygon shows the observed region. The blue x-mark shows the center of the cluster (Piffaretti et al. 2011). Red lines show the major direction and length of EIGs. Each parent name is also shown. The clouds whose parents are uncertain are labeled as "orphans."

Наличие облака в зависимости от расстояния от центра скопления

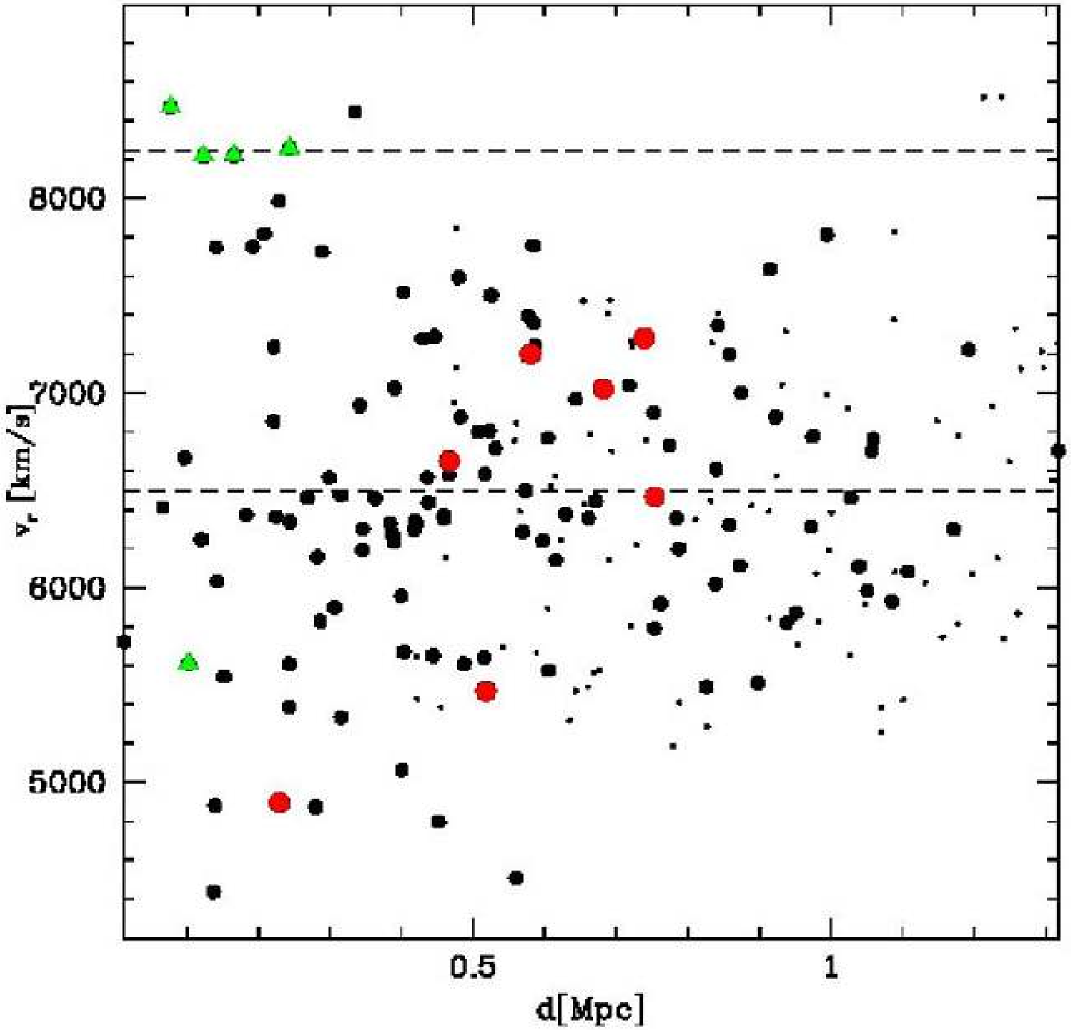

FIG. 16.— Distance from the cluster center versus recession velocity plot. The data are taken from SDSS DR12. The symbols are the same as Figure 15. Horizontal broken lines show the recession velocity of Abell 1367 (v = 6494 km s^{-1}) and BIG (v = 8244.3 km s^{-1}).

И на красной последовательности, и в голубом облаке, и между ними

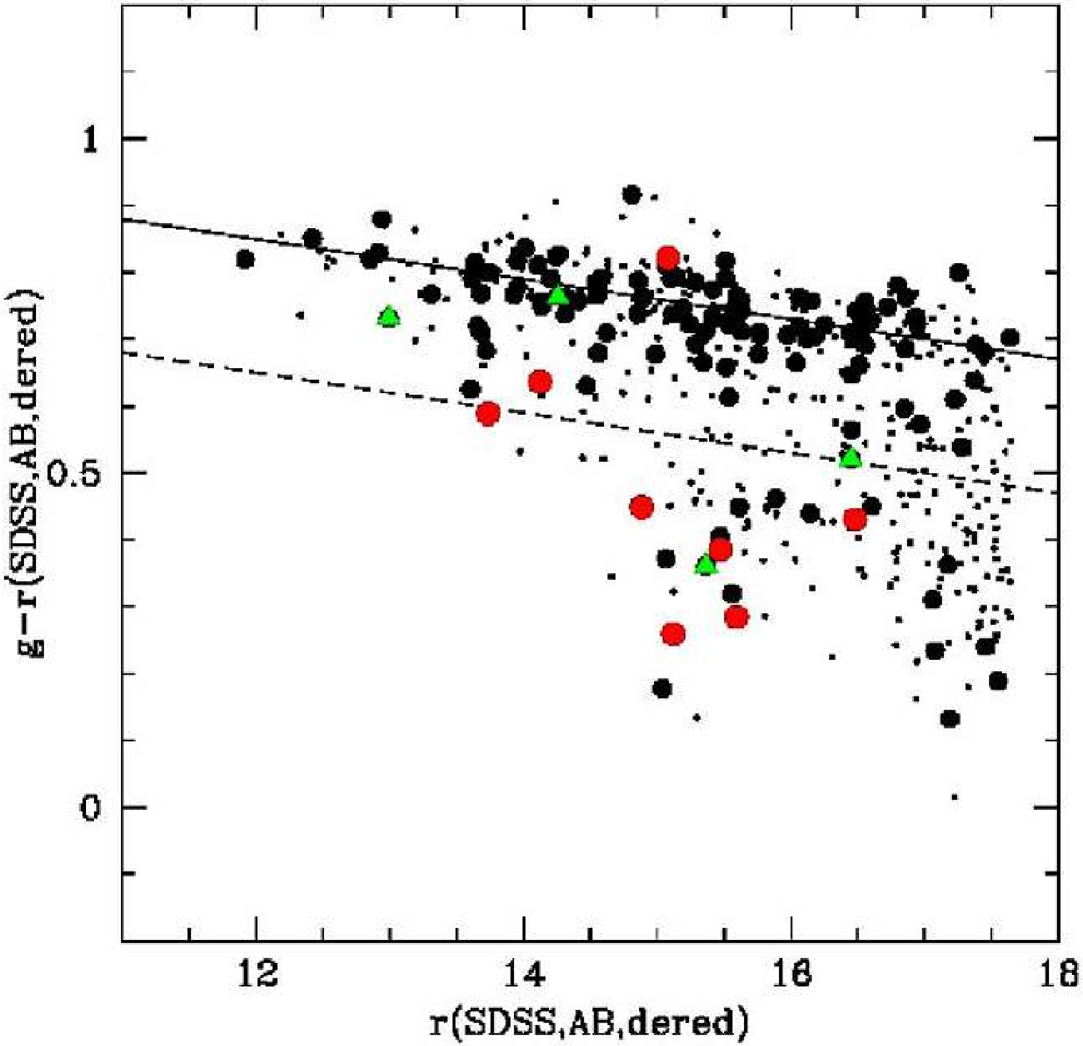

Зеленые=BIG

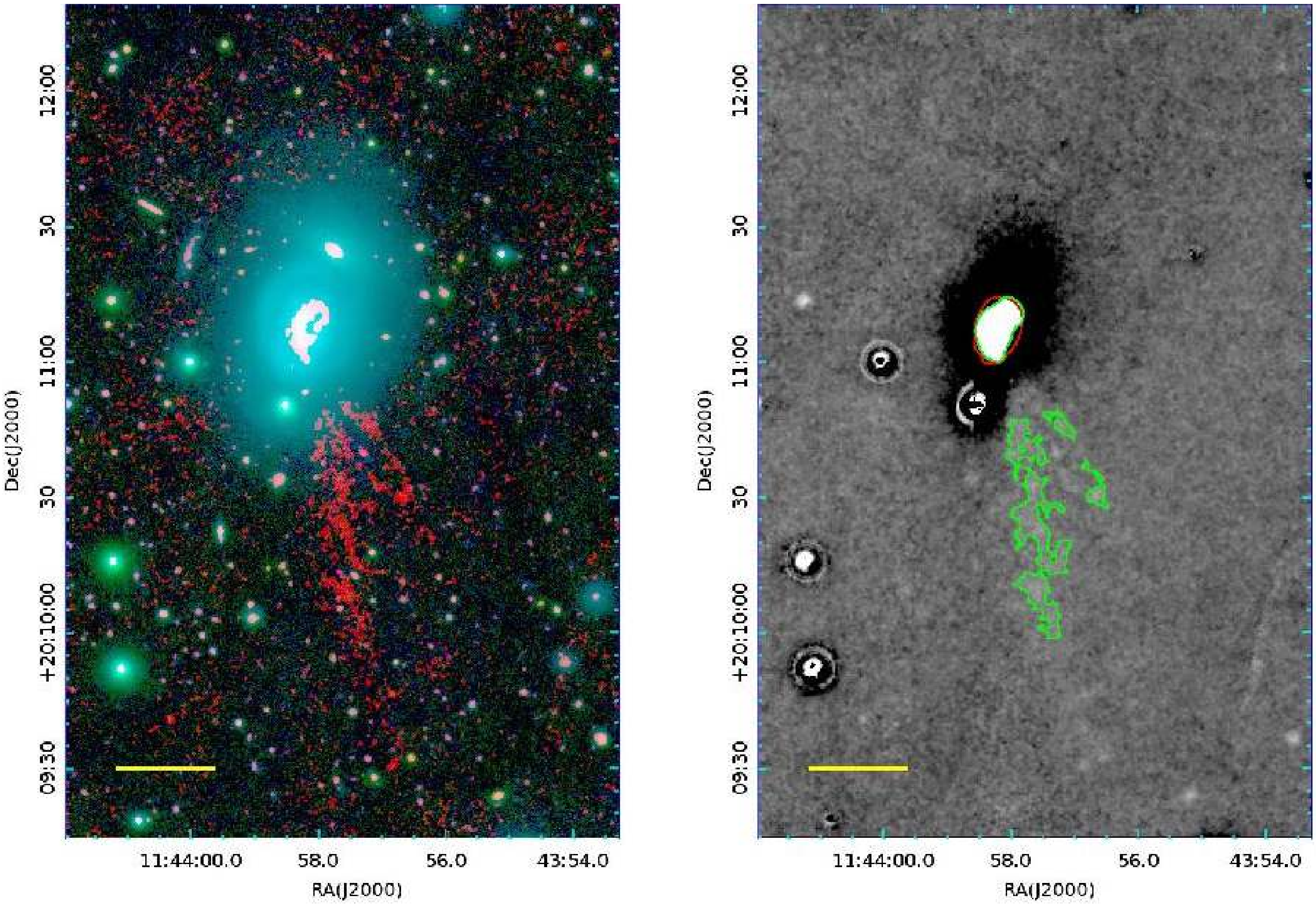
12:00
30
11:00
30
+20:10:00
09:30
Dec(J2000)
11:44:00.0
58.0
56.0
43:54.0
RA(J2000)

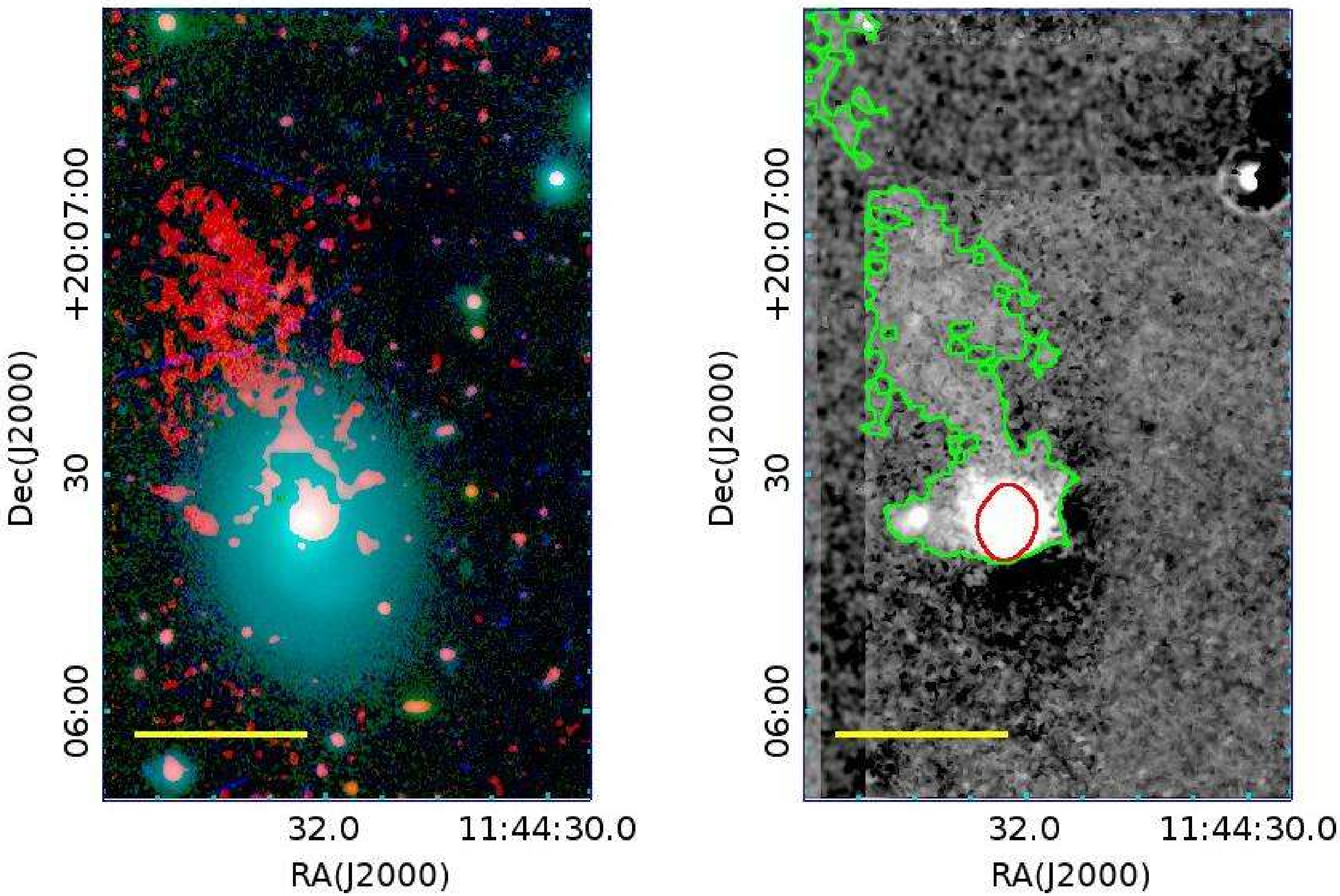

+20:07:00
30
06:00
Dec(J2000)
32.0
11:44:30.0
RA(J2000)
+20:07:00
30
06:00
Dec(J2000)
32.0
11:44:30.0
RA(J2000)

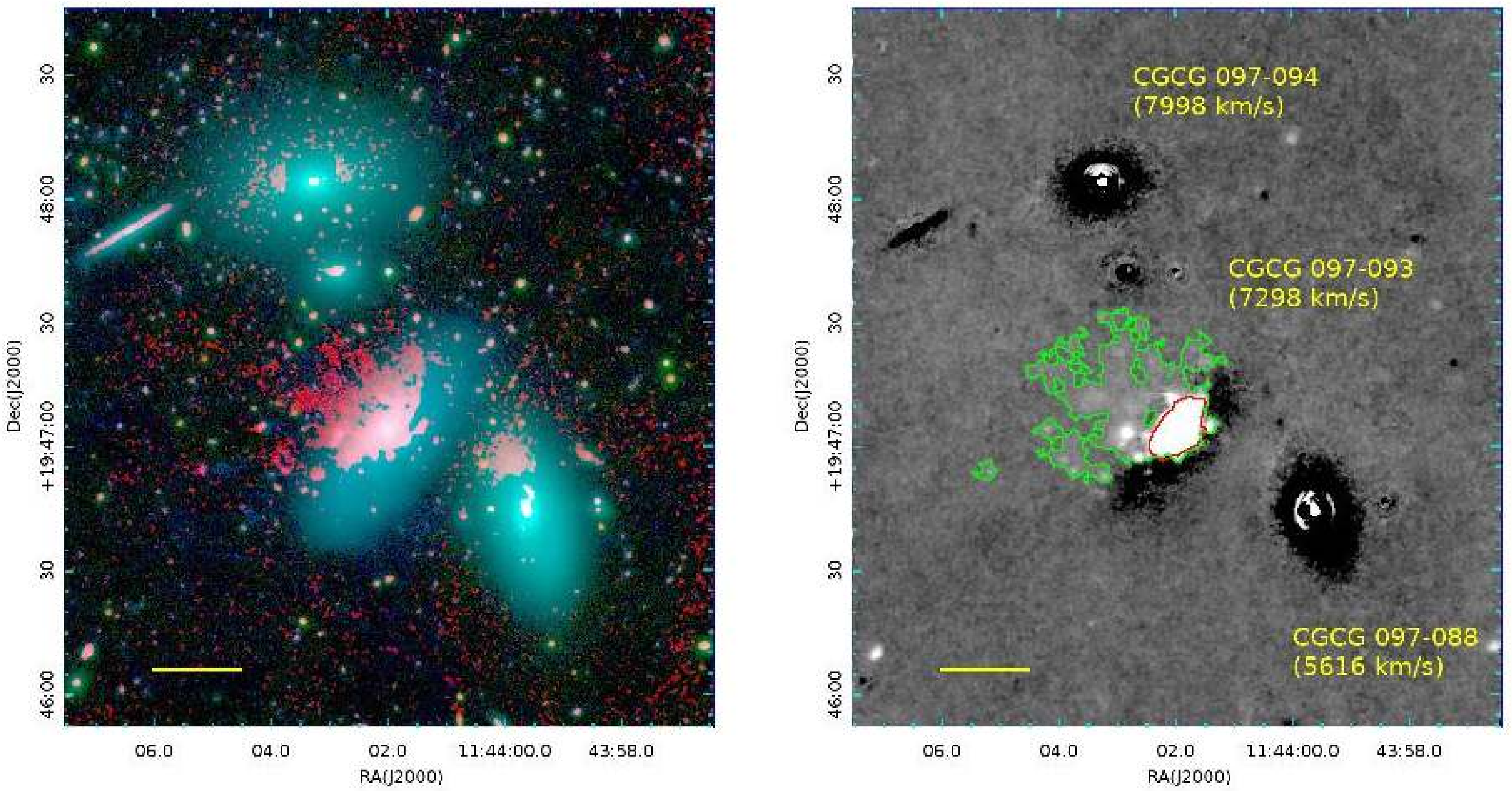

FIG. 12.— Same as Figure 8, but around CGCG 097-093. Recession velocities of three galaxies are also shown.

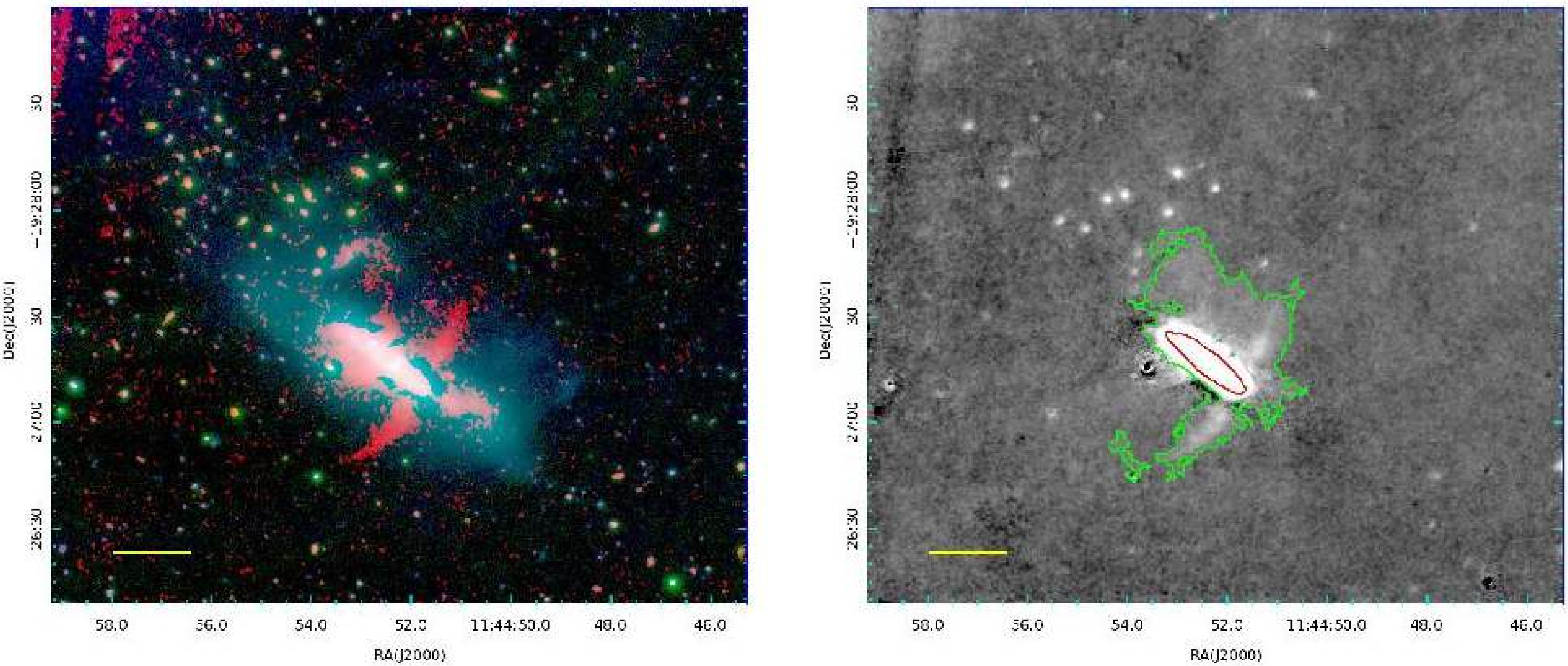

Dec(J2000)
30
−19:28:00
30
27:00
26:30
58.0
56.0
54.0
52.0
11:44:50.0
48.0
46.0
RA(J2000)

Единственный пример «облака-сиротинки» в Abell1367

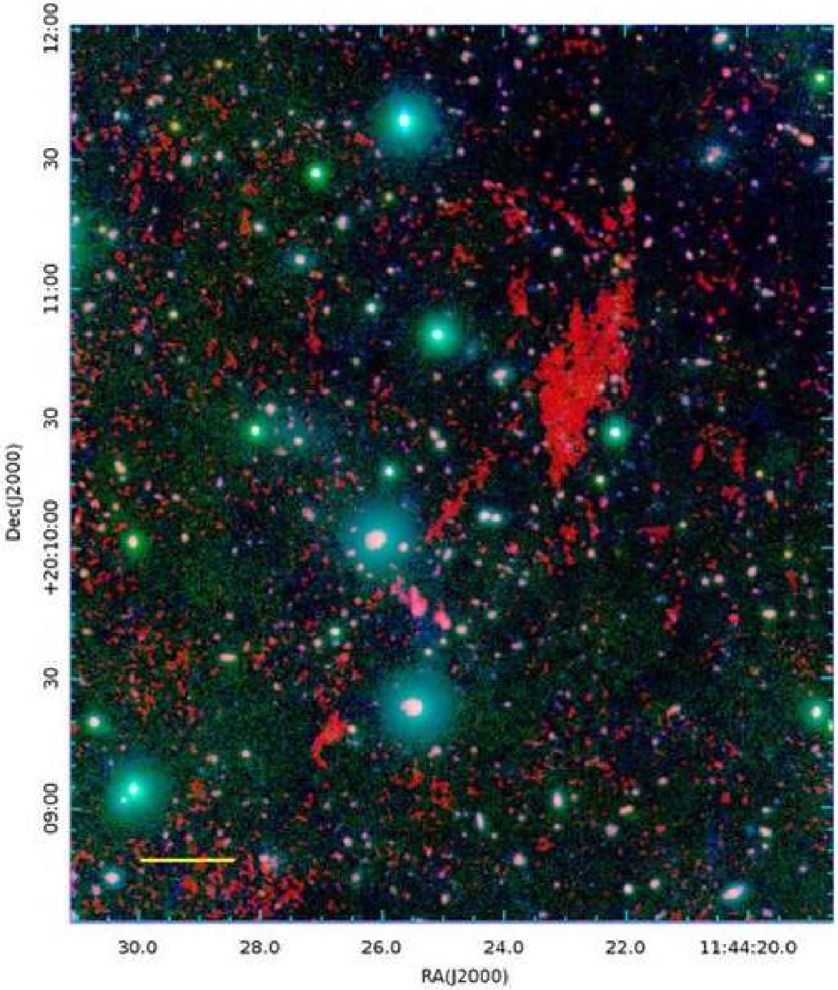

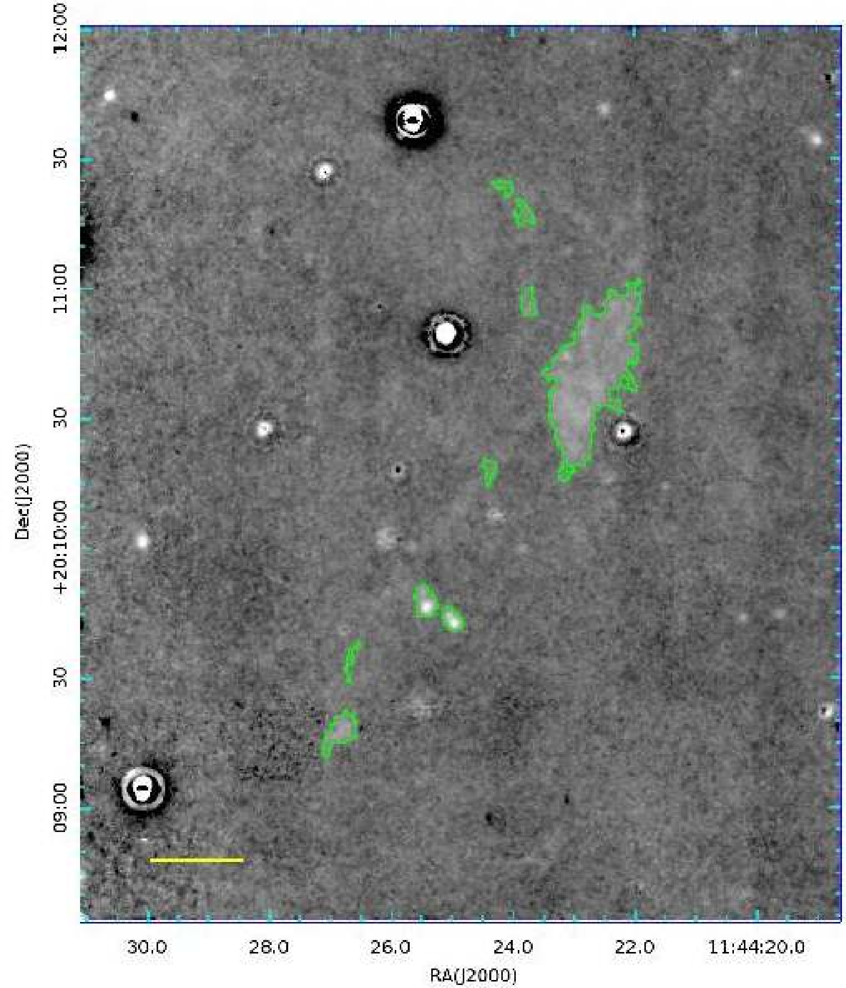

Выводы

- Сравнивая Coma и Abell1367, отмечают в последнем практически полную привязанность облаков к галактикам (в отличие от Coma); считают, что это признак динамической молодости Abell1367.